Accepted Manuscript

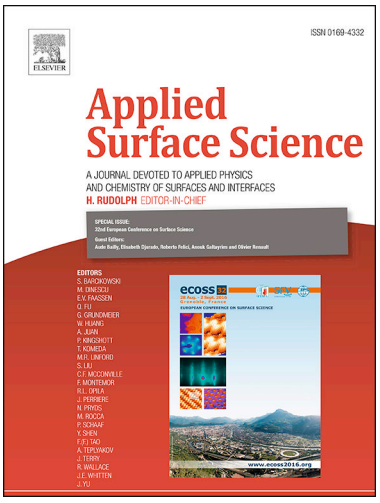

Full Length Article

Enriching the Hydrogen Storage Capacity of Carbon Nanotube Doped with Polylithiated Molecules

P. Panigrahi, S.R. Naqvi, M. Hankel, R. Ahuja, T. Hussain

PII: S0169-4332(18)30383-0
DOI: https://doi.org/10.1016/j.apsusc.2018.02.040
Reference: APSUSC 38498

To appear in: *Applied Surface Science*

Received Date: 22 December 2017
Revised Date: 31 January 2018
Accepted Date: 4 February 2018

Please cite this article as: P. Panigrahi, S.R. Naqvi, M. Hankel, R. Ahuja, T. Hussain, Enriching the Hydrogen Storage Capacity of Carbon Nanotube Doped with Polylithiated Molecules, *Applied Surface Science* (2018), doi: https://doi.org/10.1016/j.apsusc.2018.02.040

Enriching the Hydrogen Storage Capacity of Carbon Nanotube Doped with Polylithiated Molecules

P. Panigrahi[*1], S. R. Naqvi,[3] M. Hankel[2] R. Ahuja[3, 4] and T. Hussain[*2]

[1]Clean Energy and Nano Convergence Centre, Hindustan institute of Science and Technology, Chennai 603103, Tamil Nadu, India

[2] Centre for Theoretical and Computational Molecular Science, Australian Institute for Bioengineering and Nanotechnology, The University of Queensland, Brisbane, Qld 4072, Australia

[3]Condensed Matter Theory Group, Department of Physics and Astronomy, Box 516, Uppsala University, S-75120 Uppsala, Sweden

[4]Applied Materials Physics, Department of Materials and Engineering, Royal Institute of Technology (KTH), S-100 44 Stockholm, Sweden

t.hussain@uq.edu.au

akshaymitra@gmail.com

ABSTRACT

In a quest to find optimum materials for efficient storage of clean energy, we have performed first principles calculations to study the structural and energy storage properties of one-dimensional carbon nanotubes (CNTs) functionalized with polylithiated molecules (PLMs). Van der Waals corrected calculations disclosed that various PLMs like CLi, CLi_2, CLi_3, OLi, OLi_2, OLi_3, bind strongly to CNTs even at high doping concentrations ensuring a uniform distribution of dopants without forming clusters. Bader charge analysis reveals that each Li in all the PLMs attains a partial positive charge and transform into Li^+ cations. This situation allows multiple H_2 molecules adsorbed with each Li^+ through the polarization of incident H_2 molecules via electrostatic and van der Waals type of interaction. With a maximum doping concentration, that is $3CLi_2/3CLi_3$ and $3OLi_2/3OLi_3$ a maximum of 36 H_2 molecules could be adsorbed that corresponds to a reasonably high H_2 storage capacity with the adsorption energies in the range of -0.33 to -0.15 eV/H_2. This suits the ambient condition applications.

1. Introduction:

To keep the pace with the current energy crisis, there is a wide attention towards high-performance, low-cost and environmental-friendly energy conversion and storage systems. Hydrogen (H_2) is a potential energy carrier and an impeccable alternative for fossil fuel as the by-product water is ecologically harmless [1]. Though the efficiency of H_2 fuel cells is nearly two times than that of gasoline combustion engines, the major challenge rests in developing lightweight H_2 storage material at acceptable costs [2]. Hydrogen has the highest energy per mass of any fuel, but it has lowest energy per unit volume. To meet the volume restrictions in automobiles, H_2 needs storage at densities higher than its liquid density. And at the same time, for ideal room temperature desorption, the adsorption energy should be of 0.2 - 0.6 eV per H_2 [3].

So far, the developed H_2 storage technologies such as compression, liquefaction and in form of metal hydrides are not appropriate for practical application, as they need relatively high energy to store and release the H_2 and they also have issues with weight. [4] In this context, low atomic weight nanoscale carbon structures such as carbon nanotube, fullerenes, and carbon nano fibers show promise for effective H_2 storage due to their large surface to volume ratio and appear to be the potential materials for meeting U.S. Department of Energy (DOE) target of 9 wt % and 81 g/lit [5-7]. Among the carbon based nanomaterial, carbon nanotubes (CNTs) are emerging as the possible H_2 storage media. The cylindrical structure of CNT reported to increase the adsorption potential in the tube core leading to capillary forces and enhances storage capability [8]. In this regard, Dillon et al. have experimentally shown CNT to store considerable amounts of H_2 up to 5–10 wt% even at room temperature [9]. However, further studies on CNT show the interaction of H_2 with pristine CNT is van der Waals type, a very weak interaction, and cannot be considered as suitable candidate for effective H_2 storage [10,11]. Conversely, investigations on functionalized CNTs and with metal ions and adatoms have show enhanced H_2 storage capacity over pristine CNTs [12,13]. It has been reported that single walled carbon nanotube (SWCNT) with SnO_2 composite show a storage capacity of 2.4 wt % with H_2 desorption temperature in the range of 200− 350°C [14]. It has also been reported that SWCNT-WO_3 exhibits the H_2 storage capacity of 2.7 wt %, with desorption temperature range of 175− 305 ° C [15]. Whereas, CNT-TiO_2 has been

reported to exhibit H_2 storage capacity of 2.5 wt % at 25 bar and 298 K [16]. On the other hand, the first principles DFT calculation by Yildirim et al. have reported the unusual H_2 storage capacity of Ti decorated single wall carbon nanotubes [17]. The strong binding energy of H_2 to transition metals like Mg_2+ and Al_3+ has also been reported elsewhere [18]. In this regard, Aluminum hydride (AlH_3) emerges as a potential H_2 storage material due to the weak bonding of H_2 with Al clusters and the lightweight of Al [19]. This has further motivated the investigation of AlH_3 coated CNT for H_2 storage application [20].

It has been reported that in case of C_{60} fullerenes, Li atoms prefer to stay isolated and clustering of Li atoms is energetically highly unfavorable [21]. The Li atoms capped on to the pentagonal faces of the fullerene, are not only very stable but also have the binding energy of 0.075 eV per H_2 molecule for the $Li_{12}C_{60}$ cluster resulting in a high gravimetric H_2 storage capacity of 13 wt %. In the same context, Cabria et al. have studied the enhanced H_2 storage capacity of graphene and CNT while doped with Li [22]. In the same context, Chen et al have reported the enhanced binding energy of H_2 on Li-decorated CNT encapsulating the C_{60} fullerene molecule inside the nanotube [23]. The charge transfer between CNT and C_{60} promotes the charge transfer from Li to the CNT. C_{60} encapsulation in CNT results in increasing charge concentration on Li and enhances H_2 adsorption. These above studies suggest that Li might prefer to coat on CNT surface as monolayer without clustering and would open an avenue for storing hydrogen with a high storage capacity. There are several other studies, which describe the interaction of H_2 with doped NTs [24-26]

Thus, the recent research focus is on of Li-doped carbon nanostructures, where the lightweight Li^+ ion, which can bind up to $6H_2$ molecules with an average binding energy of 0.19 eV/H_2, close to the optimal binding energy per H_2. For this purpose the ionized Li need to be prevented from clustering, which results in significant hindrance in Li bonding with H_2 molecules.

In this context, the polylithiated molecules (PLMs) containing a large density of Li atoms have been identified as potential dopants on CNT for H_2 storage. The existence of the carbon-based PLMs likes CLi_5 and CLi_6 has already been experimentally confirmed [27]. Using first principles DFT calculation, Suleyman et al. have reported the PLMs likes CLi_4 and OLi_2 as the building blocks for hydrogen storage materials with calculated

gravimetric densities of 37.8 and 40.3 wt % for H_2 storage respectively [28]. In the similar context, Yunguo et al. by using DFT calculations have reported the H_2 storage capacity of 9.83 wt% for CLi_3 functionalized boron carbide (BC_3) monolayers [29]. However, the scope of CNT functionalized with PLMs for H_2 storage application is yet to be explored. Our group has extensively explored the promise of H_2 storage properties of various 2D materials functionalized with different polylithiated species [30-33] However the focus has been on 2D materials and 1D nanotubes has not be considered.

In this paper, using first principles DFT calculations, we have studied for the first time, the structure and stability of CNT functionalized with various PLMs CLi_n, n= 1-3 and OLi_m, m= 1-3 and their H_2 storage properties. We predict strong binding energy for carbon based polylithiated molecules on CNT surface than oxygen based PLMs. Our further studies revels that each Li of PLMs group functionalized on CNT can accommodate maximum of $4H_2$ molecules resulting in reasonably high H_2 storage capacity. These exceptionally high H_2 storage densities make CNT-CLi_n as fascinating building blocks for H_2 storage.

2. Computational Details:

For ground state structural optimization and energy convergence, the calculations are performed at the level of density functional theory (DFT) as implemented in the Vienna ab initio simulation package (VASP) [35,36]. In specific, we have used generalized gradient approximation (GGA) of Perdew and Wang to approximate the exchange-correlation interaction functional [37]. The projected augmented wave (PAW) method is implemented, to explicitly treat the valence electrons for Li ($1s^2 2s^1$), O ($2s^2 2p^4$), and C ($2s^2 2p^2$) [37]. The plane wave kinetic energy cutoff was optimized at 500 eV. The ground state geometries of all the structures are optimized without any symmetry constraints by using the conjugate gradient (CG) algorithm. All atomic positions and lattice parameters are optimized with convergence criterion of energy as 10^{-5} eV between two ionic steps and atomic forces are minimized with the maximum force allowed on each atom is 0.001 eV/ Å. The total energies are converged on a scale of 10-3 eV/atom. The unit cell of CNT geometry consists of 60 C atoms. The CNT structure is treated within a supercell geometry using the periodic boundary conditions. A spacing of 15 Å is maintained along

perpendicular direction of tube geometry to prevent structures from their coupling. In the self-consistent total energy calculations the Brillouin zone is sampled in the k-space within Monkhorst-Pack scheme [39] by 1×1×5. Owing to the weak H_2 binding energies with functionalized CNT, we have included van der Waals corrected interaction in our calculation as implemented with semi-empirical correction of Grimme within VASP [40]. Since aggregation of CLi_n or OLi_m molecules would be detrimental for H_2 storage, we have explored the possibilities of attaching these PLMs to CNT surface with optimum coverage effect. The aim is to immobilize the PLMs without weakening the H_2 binding to them.

The binding energies of CLi_n/OLi_m on CNT has been calculated by the following relation

$$E_b = [E (CNT- y\ CLi_n/OLi_m) – E (CNT) – y\ E (CLi_n/OLi_m)]/y \quad (1)$$

{m=n=y=1, 2, 3}

Here 1st, 2nd and 3rd terms represent the total energies of CNT loaded with PLMs, of pristine CNT and that of polylithiated CNTs respectively.

The H_2 adsorption energies has been calculated by the relation given below

$$E_{ads} = [E (CNT- CLi_n/OLi_m+zH_2) – E (CNT- CLi_n/OLi_m+ (z-1)\ H_2) – z\ E (H_2)] \quad (2)$$

In relation (2), 1st and 2nd terms represent the energies of the system loaded with zth and (z-1)th H_2 molecule. The third term represent the energy of H_2.

3. Results and Discussion:

The optimized structure of (3,3) CNT used in this study having 60 atoms is shown in fig-1. The optimized C-C bond length and C-C-C bond angle are 1.42 Å and 119.4^0 respectively, which agrees perfectly well with the literature. The interaction between the pristine CNTs and H_2 molecules are found to be negligibly small and thus needs to be improved for the ambient condition applications [41]. This weak binding could be enhanced by various means and one of the most promising techniques is doping of CNTs with foreign metals and molecules. When it comes to selecting elements for doping, specifically for H_2 storage, light elements are always preferred because of two main reasons, lightweight and lower cohesive energies. Lighter dopants are attractive in

achieving high H_2 storage capacity as compared to the heavier ones. For attaining reversibility, lower cohesive energies of the specific dopants are easy to surpass by their corresponding binding energies, which would help in getting uniform distribution of the dopants over the substrates. Alkali, alkaline and light transition metals are few of the preferred dopants for H_2 storage applications.

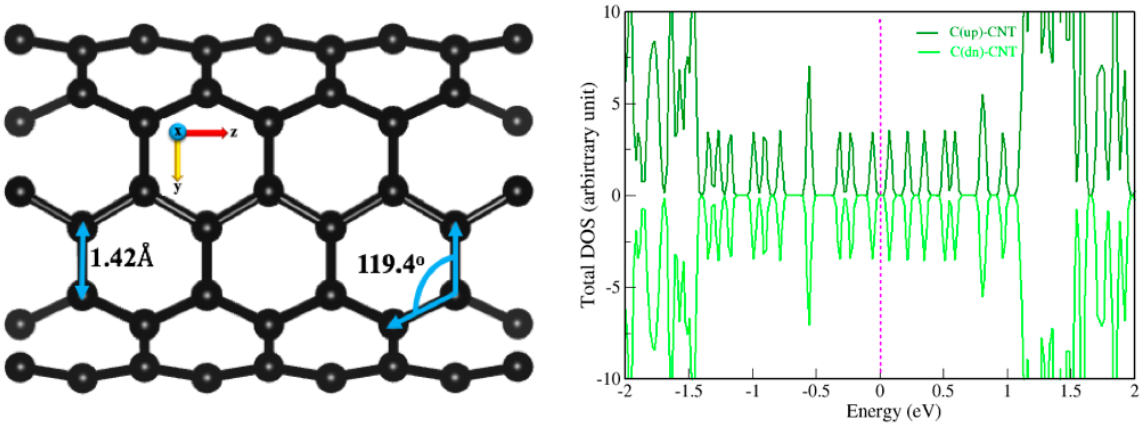

Fig. 1. (Left) Optimized structure of CNTs with bond length and bond angle of 1.42 Å and 119.4^o respectively. (Right) total DOS of pristine CNT.

Here a special class of Li rich species, PLMs, has been considered to functionalize CNTs for its application in H_2 storage. We start the doping process by introducing single member of C-based (CLi, CLi_2, CLi_3) and O-based (OLi, OLi_2 and OLi_3) polylithiated species to CNT. In order to find the most stable configuration, we explored all the possible binding sites, which are C-top, C-C bridge and hollow.

System	Binding energy per dopant E_b (eV)	CNT-Dopant average distance D (Å)	C-Li/OLi average bond length (Å)
CNT-CLi	-2.35	1.50	1.89
CNT-CLi_2	-3.61	1.55	2.03
CNT-CLi_3	-3.73	1.55	2.07
CNT-3CLi	-3.08	1.48	1.96
CNT-3CLi_2	-3.35	1.54	1.97
CNT-3CLi_3	-3.63	1.55	2.02
CNT-OLi	-2.08	1.41	1.74
CNT-OLi_2	-1.58	1.48	1.82
CNT-OLi_3	-2.06	1.90	1.70
CNT-3OLi	-2.00	1.41	1.75
CNT-3OLi_2	-1.51	1.50	1.80
CNT-3OLi_3	-1.00	1.56	1.84

Table 1. Binding energies, binding distances with CNT, bond lengths within PLMs and charge transfer between CNT and polylithiated molecules.

To preserve the reversibility of the doped systems, the PLMs should bind strongly to CNTs in such a way that there is negligibly small possibility of cluster formation. This could be achieved though strong binding between PLMs and CNTs. The binding energies (binding distances) of single molecule of both C-based PLMs on CNTs are found to be in the range -2.36 eV (1.50 Å), -3.61 eV (1.55 Å), and -3.73 eV (1.55 Å) for CLi, CLi_2 and CLi_3 respectively. Although the bindings of O-based PLMs to the CNTs are less pronounced as compared to their C-based counterparts, however these are strong enough to keep the molecules uniformly dispersed by avoiding the clustering. The calculated binding energies (binding distances) of O-Li, OLi_2 and OLi_3 are -2.08 eV (1.41 Å), -1.58 eV (1.48 Å) and -2.06 eV (1.90 Å) respectively.

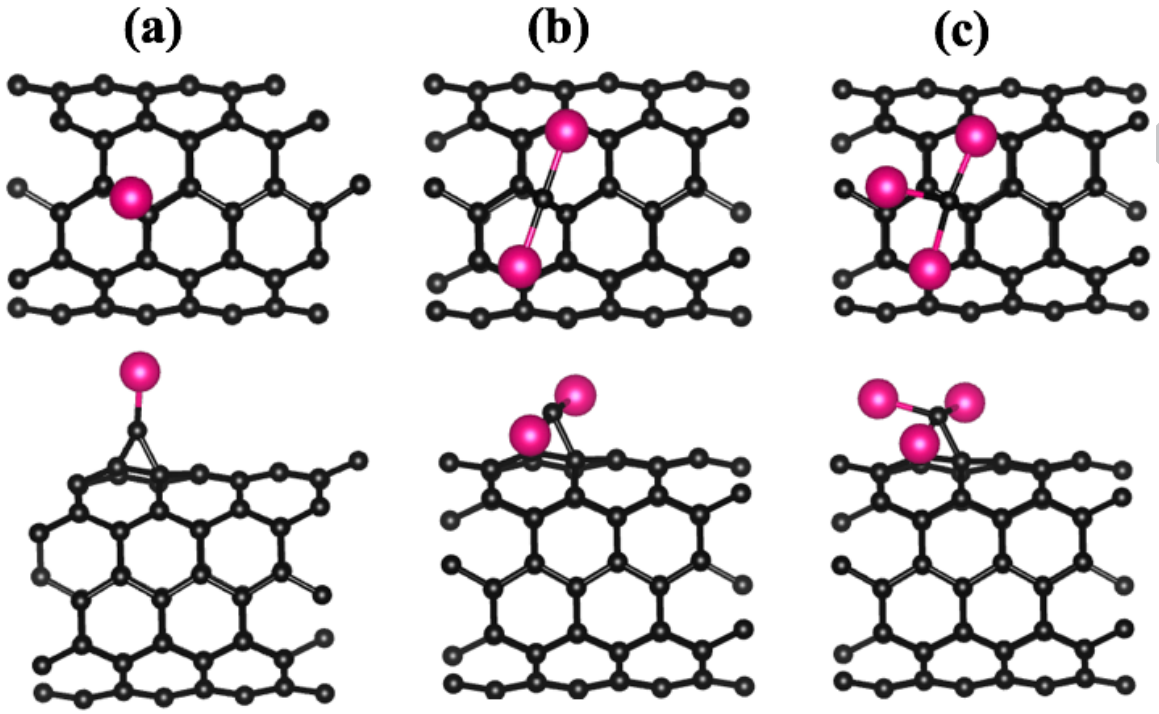

Fig. 2. Top (upper panel) and side (lower panel) views of CNTs doped with (a) CLi, (b) CLi_2, and (c) CLi_3. Black and pink balls represent C and Li atoms respectively.

Large surface area of CNTs coupled with strong bindings and relatively small binding distances of PLMs to CNTs inspired us to increase the doping concentration by introducing more PLMs, and investigate their effects on the binding characteristics. Thus we kept on putting more PLMs as long as their bindings are reasonably large to surpass the clustering effect. While introducing additional PLMs on CNTs, the same procedure of finding the most preferential binding site has been repeated by putting the former on different sites on the latter and performing the energetic analysis. It has been concluded that a maximum of three PLMs each of C-based and O-based could be attached to CNTs efficiently. At this maximum coverage the average binding energies (binding distances) per CLi, CLi_2 and CLi_3 on CNTs have been found -3.08 eV (1.48 Å), -3.35 eV (1.54 Å) and -3.63 eV (1.55 Å) respectively. For O-based PLMs, we found average binding energies (binding distances) as -2.0 eV (1.41 Å), -1.51 eV (1.50 Å) and -1.0 eV (1.56 Å) for OLi, OLi_2 and OLi_3 respectively. The optimized structures of CNTs functionalized

with both C-base and O-based PLMs are shown in fig. 3 (a, b, c) and fig. 4 (a, b, c) respectively.

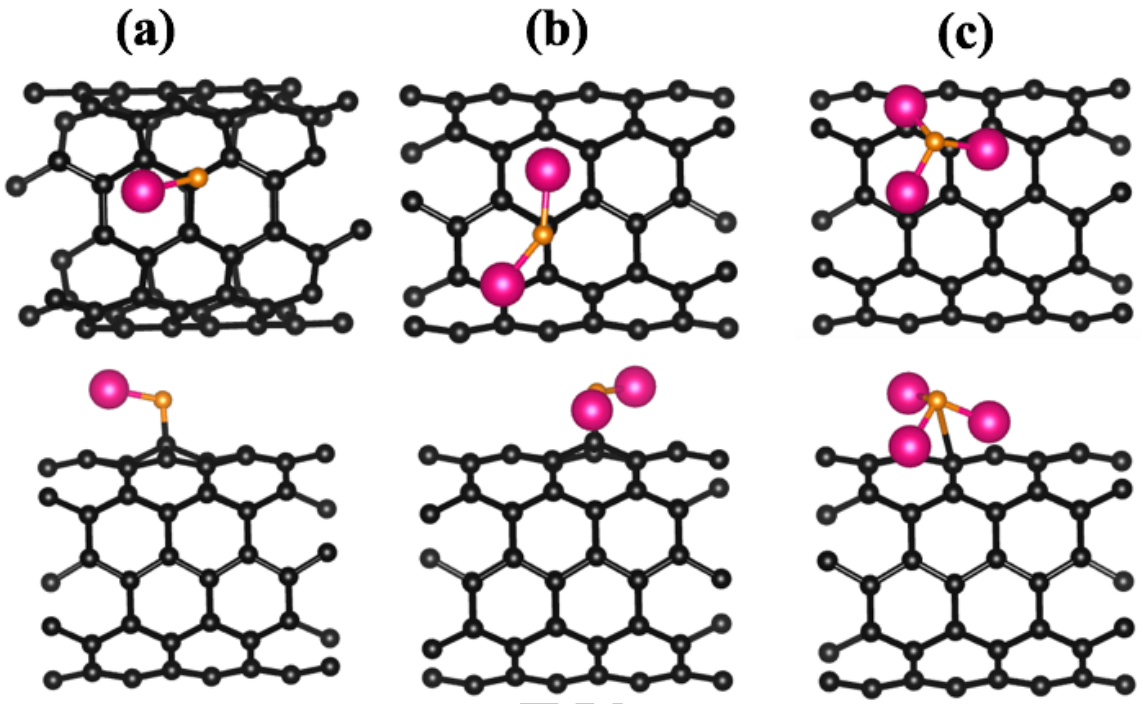

Fig. 3. Top (upper panel) and side (lower panel) views of CNTs doped with (a) OLi, (b) OLi_2, and (c) OLi_3. Black, pink and orange balls represent C, Li and O atoms, respectively.

The bonding mechanism of PLMs has been further explained by means of investigating the charge transfer mechanism through Bader analysis. Due to difference of electronegativities charge will transfer between the PLMs and CNTs. In case of C-based PLMs we explained the charge transfer by considering single PLMs for our convenience. In case of CNT-CLi structure, the Li loses significant amount of its charge (0.9e) and becomes cationic. At the same time, the C atom of CLi1 (C-CLi) loses a charge of 0.3e. Where as the C-CNT atoms gains a small charge of 0.1e and 0.05e. Here both Li and C-CLi acts as cationic groups. Where as, in CNT-CLi_2 structure, both the Li ions become cationic by loosing a charge of 0.9e. In support, the C-CLi_2, also losses a significant charge of 1.09e and becomes a cationic group. The C-CNT atoms lying in the vicinity of C-CLi_2 gain charge of 0.05e to 0.09e. In case of CNT-CLi_3 structure, each Li atoms loose charge of 0.9e where as the C-CLi_3, losses a significant amount charge of 1.1e and the C-

CL_3 group becomes strongly cationic. The C-CNT atoms in the vicinity of C-CLi_3 gain charge 0.1e.

From the bader charge analysis of optimized CNT, CNT-OLi and $OLi_,$ it is found that there is a significant charge distribution takes place in the CNT-OLi structure. The oxygen (O-OL_i) gains a charge of 0.3 e. where as the charge on Li loses a charge of 0.8e and becomes cationic. The charge of carbon atoms of CNT (C-CNT), in the vicinity of functionalized group OL, gets redistributed. Few C-CNT looses charge up to 1.01e and few gain up to 0.2e.

1. For CNT-$OLi_{2,}$ both Li atoms loose 0.08e of charge and become cationic. O-OL_1 also looses a charge of 0.6e. Where as most of the C-CNT, near to $OL_{2,}$ gains charge of nearly 0.1e.
2. In case of CNT-$OLi_{3,}$ two Li atom loose a charge of 0.08e and the 3rd Li atom loose a significant charge of 0.9e forming a strong cationic group. Where as the O atom looses a charge of 0.9e. Most of the C-CNT, near to $OL_{3,}$ gains charge of nearly 0.1e.

   The transfer and accumulation of charge can been seen though electron density plots as shown in fig. 4 of both C-based and O-based PLMs functionalized CNTs

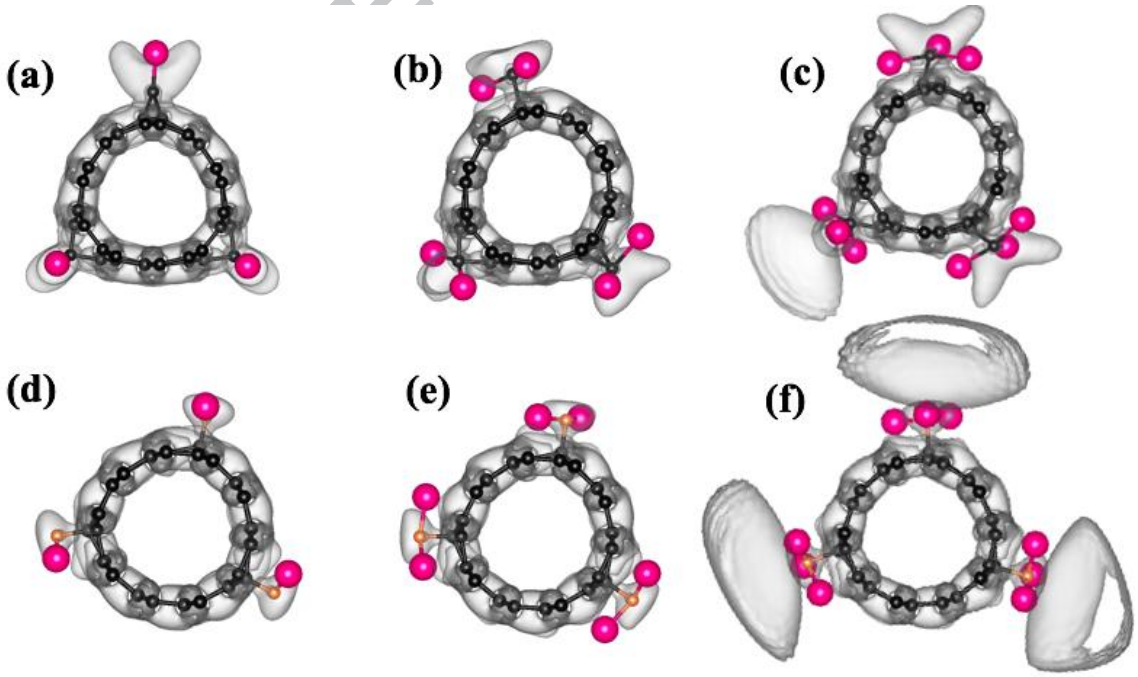

Fig. 4. Electron density plots of (a) CLi-CNT, (b) CLi_2-CNT, (c) CLi_3-CNT, (d) OLi-CNT, (e) OLi_2-CNT, and (f) OLI_3-CNT. The isosurface level is set to 0.4 e/bohr^3. Black, pink and orange balls represent C, Li, and O atoms. Electron clouds are indicated as grey areas in the figures.

Electronic Density Of States:

From the total DOS plots of CNT, we see CNT is a no-band gap non-magnetic system as can be seen in fig (1). From partial density of states (PDOS) plots of CLi-CNT, we find a strong hybridization between Li(s) of CLi_1 with that of C (p) of CNT fig.5 (a). In case of CLi_2-CNT, there is a strong hybridization between C(p)-CNT with that of C(p)-CLi_2 near the Fermi energy fig. 5 (b).

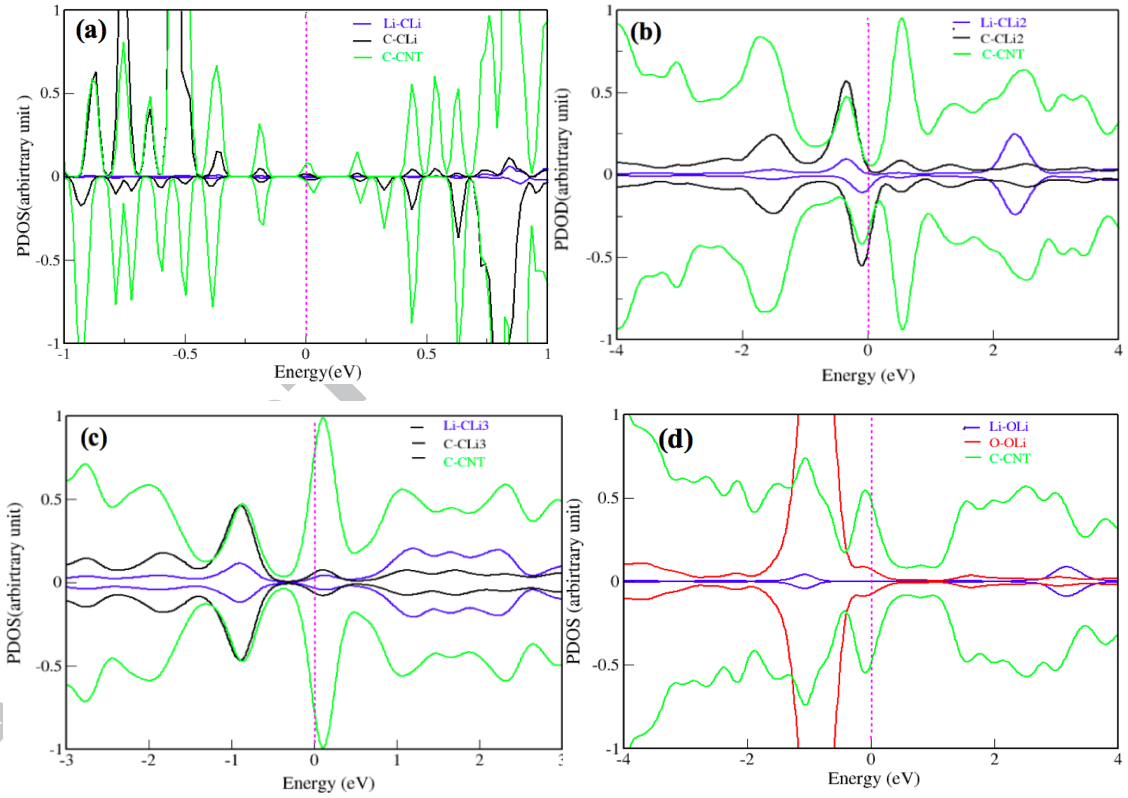

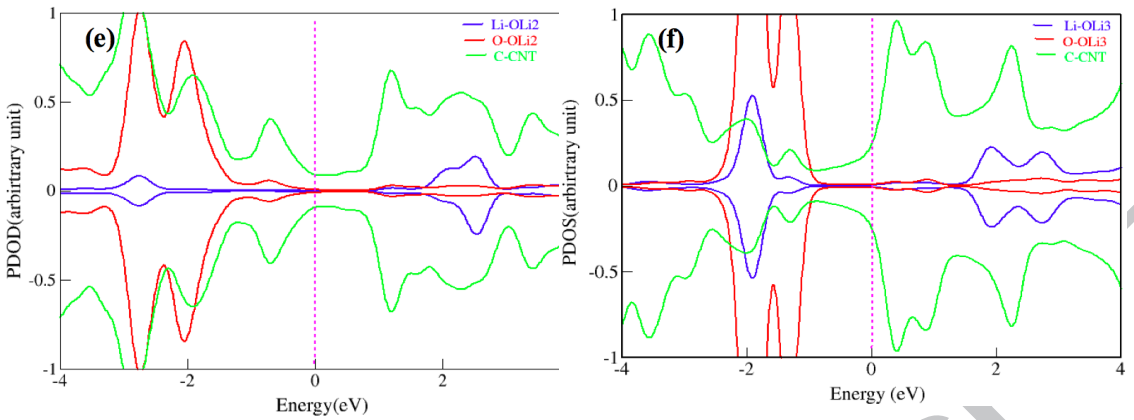

Fig. 5. PDOS plots for (a) CLi, (b) CLi2, (c) CLi3, (d) OLi, (e) OLi2, and (f) OLi3 doped CNTs.

In case of CLi_3-CNT, the hybridization is strong between C (p)-CNT with that of C (p)-CLi_3 and Li(s)-CLi_3 near the Fermi energy, as shown in fig. 5 (c) which explains the strong binding (3 eV) of CLi_m group to the CNT surface.

Where as from the partial density of states (PDOS) plots of OLi_i-CNT, we find, the hybridization between OLi_m to CNT is rather weaker compared that with CLi_n group. We can see from the PDOS plot Fig. 5 (a, b, c) the electronic states at the Fermi energy are mostly dominated by C(p) states of CNT. In case of OLi_1–CNT, there is a small hybridization between (fig a), C(p)-CNT with that of O(p)- OLi_1, giving a binding energy of (2 eV) near the Fermi energy. However, there is little bonding between OLi_m (m=2,3) and CNTs as evident at the Fermi energy in Fig. 5 (e, f), which explains the low binding energy of 1.5 eV and 1 eV for OLi_2 and OLi_3 to CNT.

Hydrogenation:

In this section of the manuscript, we will discuss in detail the hydrogenation mechanism and H_2 storage capacity of PLMs functionalized CNTs at maximum doping concentration. As mentioned in charge analysis section that each Li of both C-based and O-based PLMs acquires a partial positive charge through donating a fraction of its valence charge to C/O atom of PLMs it is attached to. This situation leaves multiple Li^+ cations around each PLM bonded to CNTs. Now the incident H_2 molecules, which are to be stored, approach the functionalized PLMs and get polarized due to the presence of Li^+ cations. Here we have considered different adsorption configurations of H_2 molecules by

exposing them vertically, horizontally and tilted to Li^+ cations. The most preferred configuration is vertical H_2 adsorption, which corresponds to the lowest energy. Apart from being energetically favorable, it would also allow multiple H_2 to be adsorbed around each Li^+ cations and hence yield maximum H_2 storage capacity.

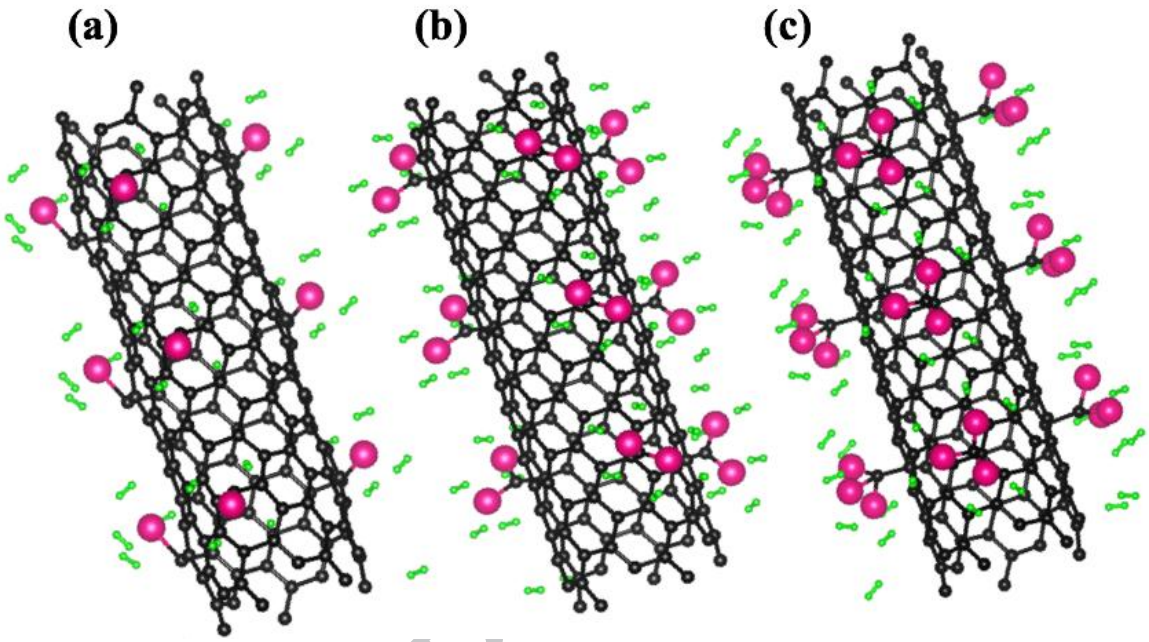

Fig. 6. Hydrogenated (a) CLi-CNT, (b) CLi_2-CNT, and CLi_3-CNT. Black, pink and green balls represent C, Li and H atoms, respectively.

The adsorption process will proceed with one H_2 molecule on each Li^+ cation and allowing the system to relax completely. This optimized structure with H_2 molecule adsorbed will be a starting structure for the adsorption of next H_2 and the system undergoes complete optimizations again. This process will continue until the system reaches to saturation where further exposure of H_2 becomes difficult due to the repulsion of already adsorbed H_2 molecules, which are polarized by Li^+ cations.

It has been observed that a total of $24H_2$, $36H_2$ and $36H_2$ could be adsorbed on CNT-3CLi/3OLi, CNT-$3CLi_2$/$3OLi_2$ and CNT-$3CLi_3$/$3OLi_3$ respectively. The average adsorption energies per H_2 range between -0.33 eV to -0.15 eV, which is perfect for the ambient condition utilization. The optimized structures of C-based and O-based PLMs

functionalized CNTs upon maximum hydrogenation are shown in fig. 6 (a, b, c) and fig. 7 (a, b, c) respectively.

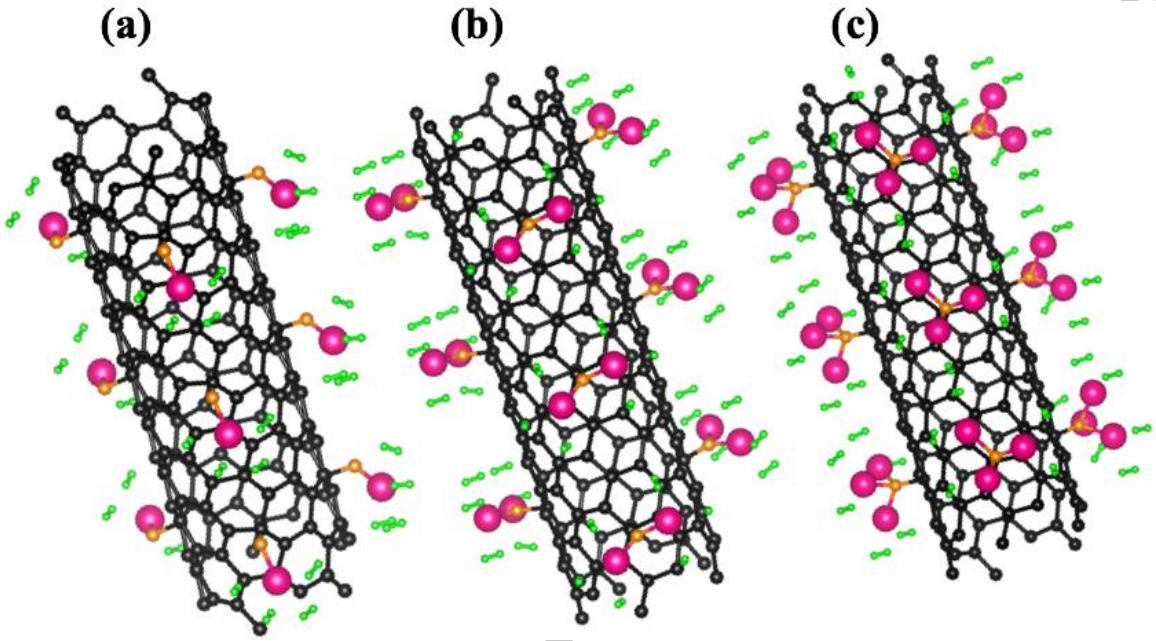

Fig. 7. Hydrogenated (a) OLi-CNT, (b) OLi_2-CNT, and OLi_3-CNT. Black, pink, orange and green balls represent C, Li, O and H atoms, respectively.

4. Conclusion:

In this study we have used first principles calculations based on DFT to investigate the structural, electronic, charge transfer and H_2 storage properties of various C and O-based PLMs functionalized CNTs. The PLMs considered here includes CLi, CLi_2, CLi_3, OLi, OLi_2, and OLi_3 at varied doping concentrations. Our van der Waals corrected computations suggested that even a high doping concentration all the studied PLMs CLi (OLi), CLi_2 (OLi_2) and CLi_3 (OLi_3) bind with CNTs with average binding energies of -3.08 (-2.0), -3.35 (-1.51) and -3.63 eV (-1.0 eV) respectively. This high binding would help uniform distribution of the PLMs over the CNT without forming the clusters, which would have halted the reversibility and H_2 storage capacity significantly. Upon doping there is exchange of charge not only between the CNT and PLMs but also within PLMs,

which would leave all the Li to gain partial positive charge though donation of some its valence electrons. The cationic nature of Li^+ proves very beneficial in anchoring multiple H_2 molecules with binding energies that falls between chemisorption and physisorption. Multiple PLMs doped on CNT could achieve a significantly high H_2 storage capacity and prove to be an efficient storage medium for clean energy.

Acknowledgements

We are indebted to the CENCON, Swedish Research Council (VR), Carl Tryggers Stiftelse för Vetenskaplig Forskning for financial support. The SNIC and UPPMAX are also acknowledged for provided computing time. We are thankful to UQ for providing the financial support and the resources at NCI National Facility systems at the Australian National University through National Computational Merit Allocation Scheme supported by the Australian Government and the University of Queensland Research Computing Centre.

References:

1. G. W. Crabtree, M. S. Dresselhaus, M. V. Buchanan, Phys. Today 57 (2004) 39−44.
2. J. Tollefson, J. Nature, 464 (2010) 1262−1264.
3. A. Sigas, M. I. Rojas, E. P. M. Leiva, Int. J. Hydrogen Energy 36 (2011) 3537−3546.
4. T. Hussain, M. S. Islam, G. S. Rao, P. Panigrahi, D. Gupta and R. Ahuja, Nanotechnology 26 (2015) 275401-275406.
5. C. Liu, Y. Y. Fan, M. Liu, H. T. Cong, H. M. Cheng, M. S. Dresselhaus, Science 286 (1999) 1127−1129.
6. H. M. Cheng, C. Liu, Y. Y. Fan, F. Li, G. Su, H. T. Cong, L. L. He, M. Liu, Z Metallkd. 91 (2000) 306−410.
7. C. C. Ahn, Y. Ye, B. V. Ratnakumar, C. Witham, R. C. Bowman Jr, B. Fultz, Appl. Phys. Lett. 73 (1998) 3378−3380.
8. Y. Ye, C. C. Ahn, C. Witham, B. Fultz, Appl. Phys. Lett. 74 (1999) 2307−2309.
9. A. C. Dillon, K. M. Jones, T. A. Bekkendahl, C. H. Kiang, D. S. Bethune, M. J. Heben, Nature 386 (1997) 377−379.

10. M. Rzepka, P. J. Lamp, J. Phys. Chem. B 102 (1998) 10894−10898.
11. G. G. Tibbetts, G. P. Meisner, C. H. Olk, Carbon 39 (2001) 2291−2301.
12. H. S. Kim, H. Lee, K. S. Han, J. H. Kim, M. S. Song, M. S. Park, J. Y. Lee, J. K. Kang, J. Phys. Chem. B 109 (2005) 8983−8986.
13. L. Chen, Y. M. Zhang, N. Koratkar, P. Jena, S. K. Nayak, Phys. Rev. B 77 (2008) 033405.
14. D. Silambarasan, V. J. Surya, V. Vasu, K. Iyakutti, Int. J. Hydrogen Energy 38 (2013) 4011−4016.
15. D. Silambarasan, V. J. Surya, V. Vasu, K. Iyakutti, T. R. Ravindran, Int. J. Hydrogen Energy, submitted for publication.
16. A. Mishra, S. Banerjee, S. K. Mohapatra, O. A. Graeve, M. Misra, Nanotechnology 19 (2008) 445607.
17. T. Yildirim, S. Ciraci, Phys. Rev. Lett. 94 (2005) 175501.
18. R. C. Lochan, M. H. Gordon, Phys. Chem. Chem. Phys. 8 (2006) 1357–1370.
19. H. Kawamura, V. Kumar, Q. Sun, Y. Kawazoe, Phys. Rev. A 67 (2003) 063205.
20. K. Iyakutti, Y. Kawazoe, M. Rajarajeswari, V. J. Surya, Int. J. Hydrogen Energy 34 (2009) 3 7 0 – 3 7 5.
21. Q. Sun, P. Jena, Q. Wang, M. Marquez, J. Am. Chem. Soc. 128 (2006) 9741−9745.
22. I. Cabria, M. J. Lopez, J. Chem. Phys. 123 (2005) 204721.
23. L. Chen, Y. Zhang, N. Koratkar, P. Jena, S. K. Nayak, Phys. Rev. B 77 (2008) 033405.
24. M. Samadizadeh, A. A. Peyghan, F. S. Rastegar, Main Group Chem. 15 (2), (2016) 107-116.
25. J. Beheshtian, A. A. Peyghan, J. Mol. Model. 19 (2012) 255-261.
26. J. Beheshtian, H. Soleymanabadi, M. Kamfiroozi, A. Ahmadi, J. Mol. Model. 18 (2012) 2343-2348
27. H. Kudo, Nature 355 (1992) 432–434.
28. S. Er, A. de W. Gilles, B. Geert, J. Phys. Chem. C 113 (2009) 8997–9002.
29. Y. Li, T. Hussain, A. D. Sarkar, R. Ahuja, Solid State Commun. 170 (2013) 39–43.

30. T. Hussain, T. Kaewmaraya, M. Hankel and V. Amornkitbamrung, App. Sur. Sci. 419 (2017) 708-712.
31. S. R. Naqvi, G. S. Rao, W. Luo, R. Ahuja and T. Hussain, ChemPhysChem 18 (2017) 513-518.
32. T. Hussain, S. Chakraborty, T. W. Kang, B. Johansson and R. Ahuja, ChemPhysChem 16 (2015) 634-639.
33. T. Hussain, A. De Sarkar and R. Ahuja, Int. J. Hyd. Energy, 39 (2014) 2560-2566.
34. T. Hussain, T. A. Maark, A. De Sarkar and R. Ahuja, App. Phys. Lett. 101, 243902 (2012)
35. G. Kresse, J. Hafner, Phys. Rev. B 47 (1993) 558.
36. G. Kresse, J. Hafner, Phys. Rev. B 49 (1994) 14251.
37. J. P. Perdew, K. Burke, M. Ernzerhof, Phys. Rev. Lett. 77 (1996) 3865.
38. P. E. Blochl, Phys. Rev. B 50 (1994) 17953.
39. H. J. Monkhorst, J. D. Pack, Phys. Rev. B 13 (1976) 5188.
40. S. Grimme, J. Comput. Chem. 27 (2006) 1787−1799.
41. G. G. Tibbetts, G. P. Meisner, C. H. Olk, Carbon 39 (2001) 2291−2301

Highlights:

1. Functionalization of carbon nanotubes with polylithiated molecules
2. Determination of structural and electronic properties
3. Charge transfer mechanism through bader analysis
4. Hydrogen storage characteristics of the functionalized systems